A Shadow-Rate Term Structure Model for the Euro Area *

Wolfgang Lemke† Andreea Liliana Vladu‡

First preliminary version
September 7, 2014

Abstract

We model the dynamics of the euro area yield curve using a shadow-rate term structure model (SRTSM), with particular attention to the period since late 2011 when interest rates have been at the lowest level since the inception of EMU. The shadow rate is driven by latent factors with linear Gaussian dynamics, while the actual short rate is the maximum between the shadow rate and a lower bound (estimated at 10 bps) so that interest rates will never fall below that level. The estimated SRTSM performs attractively with respect to cross-sectional fit and forecast performance. The model implies that since mid-2012 the median horizon when future one-month rates would return to 50 bps has been ranging between about 25 and 40 months. Deriving such lift-off timing instead from the simple metric of the forward curve crossing 50 bps would underestimate the SRTSM-implied median timing by between 5 to 15 months. As a novelty in the literature, we analyze the effect of a downward shift in the lower bound on the yield curve: for short maturities, rates decrease one-to-one with a drop in the lower bound, while the effect diminishes for longer maturities. The shift-down in the euro area yield curve between April and June 2014 appears to partially reflect such a drop in the (perceived) lower bound.

Keywords: term structure of interest rates, lower bound, nonlinear state space model, monetary policy expectations

*We thank Hans Dewachter, Peter Hoerdahl and Christian Schlag, as well as seminar participants at the ECB, the Bundesbank and the Goethe University Finance Brown Bag seminars for helpful comments and discussions. The views expressed are those of the authors and do not necessarily reflect those of the European Central Bank or the Deutsche Bundesbank.

†European Central Bank, Kaiserstrasse 29, D-60311 Frankfurt am Main, Germany, wolfgang.lemke@ecb.int, corresponding author

‡Deutsche Bundesbank and Johann Wolfgang Goethe University, Frankfurt am Main, andreea.liliana.vladu@bundesbank.de

1 Introduction

We model the dynamics of the term structure of interest rates in the euro area, paying particular attention to the period since late 2011 when interest rates have been at the lowest level since the inception of Economic and Monetary Union in 1999. The phenomenon of interest rates reaching historically low levels was of course not unique to the euro area, but has been rather observed in several industrialized economies, where, in fact, rates had reached a level near zero already earlier. For instance, the US effective Federal funds rate reached a level below 0.2 percent at the end of 2008 and stayed there since then, while in Japan, the period of very low interest rates has even started in the early 2000s already.

The low-rate environment poses a challenge for several of the commonly used term structure models. For instance, at rate levels near zero, models from the popular class of Gaussian affine term structure models (ATSMs) would typically imply significant probabilities of short-term rates going significantly into negative territory. This would in turn affect model-based decompositions into expectations and term premia. More generally, linear Gaussian models fail to pay due account to the inherent asymmetry in a low-rate environment, where interest rates have considerable scope to rise, but only limited, if any, room to decrease further.

This has spawned a large body of literature that proposes models to capture the specific properties of the yield curve in a low-rate environment. Most of these models incorporate a lower bound on rates, where this lower limit is often assumed to be zero. Within the group of models that incorporate such a lower bound, the class of so-called shadow-rate models have become particularly prominent.[1] They incorporate linear Gaussian factor dynamics as driving forces – exactly like in Gaussian ATSMs– but it is the 'shadow rate' s_t rather than the actual short-term rate r_t which is driven by those factors. Actual short rates are given as $r_t = max\{s_t, r_{LB}\}$, i.e. they equal the shadow rate, if this is above the bound r_{LB}, while actual rates are stuck at r_{LB}, if the shadow rate is below that bound.

The concept of a shadow-rate process was originally introduced by Black (1995). An early application is Bomfim (2003) who uses a shadow-rate term structure model (SRTSM) to estimate the probability of the Federal Funds Rate hitting the zero lower bound in 2002 and early 2003. Most other early applications were on Japan. For instance, Ueno, Baba, and Sakurai (2006) employ the solutions for a one-factor SRTSM derived by Gorovoi and Linetsky (2004) on Japanese Government Bonds (JGBs) to infer market expectations of the ending time of the Bank of Japan's zero interest rate policy. Using a more flexible two-

[1] Other types of models that accommodate a lower bound on interest rates are multifactor Cox-Ingersoll-Ross models and quadratic-Gaussian models analysed in Kim and Singleton (2012) and Kim (2008) and Andreasen and Meldrum (2013). There are also novel models being proposed, e.g. the new class of affine term structure models with non-negative short rates of Monfort, Pegoraro, Renne, and Roussellet (2014) and the class of linear-rational term structure models of Filipovic, Larsson, and Trolle (2014).

factor model with macro variables and survey forecasts, Ichiue and Ueno (2007) analyse the equilibrium interest rate in Japan. Ichiue and Ueno (2006) were also the first to estimate a macro-finance two-factor shadow-rate term structure model for Japan, pointing to the difficulties faced by a central bank to control real rates in a zero nominal rates environment. Kim and Singleton (2012) estimate two-factor shadow-rate models and demonstrate their better performance in capturing the features of the JGBs data relative to multifactor Cox-Ingersoll-Ross and quadratic-Gaussian models. Christensen and Rudebusch (2014) show the disagreement for the shadow-rate process across models with a different number of factors estimated on JGBs using the continuous-approximation of Krippner (2012). Focusing on the recent US experience with very low interest rates, Bauer and Rudebusch (2013) demonstrate better performance of both latent-factor and macro-finance shadow-rate models over ATSMs in capturing key features of the term structure in a low-rate environment. Kim and Priebsch (2013) estimate a shadow-rate term structure model enhanced with survey forecasts using the approximation in continuous time proposed by Priebsch (2013). Wu and Xia (2014) derive an approximation of forward rates in discrete time shadow-rate models and employ it to assess the effects of the US unconventional monetary policy at the zero lower bound.

To our knowledge, this paper is [one of] the first to apply the shadow-rate approach to euro area data. For estimation, we follow the approach of Bauer and Rudebusch (2013): first, following the method expounded in Joslin, Singleton, and Zhu (2011), we estimate a standard Gaussian ATSM over the period from 1999 to September 2011, a time where lower-bound considerations were largely irrelevant; second, based on the parameters obtained in the first step, we use the extended Kalman filter over the months from October 2011 to April 2014 ('lower bound' period) to filter out the driving forces of the term structure under the constraint of a lower bound prevailing. The yield curve in our analysis is derived from EONIA swap rates with maturities between three months and ten years.

Unlike Bauer and Rudebusch (2013) in their US application, though, we do not assume the lower bound r_{LB} to be zero but rather treat it as a free parameter, for which we obtain an estimate of 10 basis points. In fact, during the considered lower-bound period, the mode of the empirical short rate distribution was around 10 bps, but short-term interest rates were occasionally below the 10-bps level (and likewise above it). Hence, from the viewpoint of the model, the 10-bps bound may be interpreted as an 'elastic bound', and we refer to our estimate as the 'effective lower bound'.

We find that the estimated shadow-rate term structure model performs attractively with respect to the euro area yield curve data in several dimensions: first, the cross-sectional fit is good (with an error standard deviation of about 3-4 bps) and very much comparable to the Gaussian model, both for the for the lower-bound period and for the time before. Second, the shadow-rate model tends to overall improve upon the forecast performance of its affine Gaussian counterpart during the lower-bound period, especially

for shorter maturities and for shorter forecast horizons. Third, the Gaussian model tends to produce forecasts of distinctly – and, arguably, 'unrealistic' – negative interest rates during the lower-bound period, which in turn implies sizeable estimated forward premia over shorter horizons. The shadow-rate model avoids such implausible forecasts, and forward premia for the lower-bound period turn out to be near zero. Term premia for longer horizons, by contrast, are roughly similar across the two model classes, reflecting the fact that for longer maturities the relevance of a lower bound tends to diminish.

Similar to Bauer and Rudebusch (2013), we deploy the model to analyze interest rate expectations, the most likely interest rate path (i.e. the mode of the model-implied future rate path) and the term-structure-implied timing when rates will depart from the lower bound and pass a certain hurdle of, say, 50 bps. We find that since mid-2012 the estimated median timing when future one-month rates would return to 50 bps has been ranging between about 25 and 40 months. By contrast, a corresponding simple metric implied by the respective forward curve crossing that level has always implied an earlier timing of between 5 to 15 months before the model-implied median date.

Overall, the model (with the estimated effective lower bound of 10 bps) seems to adequately capture term structure dynamics until April 2014, the end of our estimation sample. However, following the ECB interest rate cut in June 2014, where the deposit facility rate (one of the key ECB policy rates) was for the first time decreased to a negative level of -10 bps, it turns out that the lower bound of 10 bps seems no longer adequate and needs to be reduced to account for the yield curve shapes observed since June. Such a situation where the lower bound itself seems to have been shifted is a novel constellation, which has not been addressed in the literature on the term structure at the lower-bound before.

In light of that phenomenon, we analyze further how the term structure of interest rates reacts to a change in the lower bound, using the forward curve approximation by Wu and Xia (2014). As a result of this comparative statics exercise, we find that the effect of a 'shock to the lower bound' depends on the initial constellation of the yield curve: when the shadow rate is deeply negative and short-term rates are at the lower bound, a shift in the lower bound affects the short end of the curve almost one for one, while the impact diminishes when moving further out along the maturity spectrum. By contrast, when rates are at average levels, a shock to the lower bound has only a negligible impact on the curve. Finally, we use the model to decompose the total change in the yield curve between April and June 2014, into a part which is due to a shift in the lower bound and another part, which is attributed to changing risk factors. It turns out that the change in the lower bound alone accounts for the downward shift in the yield curve until maturities of about 1.5 years, while for higher maturities changing risk factors account for the bulk of rate decreases.

2 The model

We employ a latent-factor arbitrage-free term structure model in discrete time, with linear Gaussian factor dynamics and a nonlinear mapping between factors and the short-term (i.e. one-period) interest rate, which makes sure that the short rate will not fall below some lower bound. Bond yields are risk-neutral expectations of average future short rates. Throughout, the periodicity should be thought of as monthly in line with our empirical set-up, and the interest rate with shortest maturity is the one-month rate.

Specifically, under the physical ('real-world') measure $\mathbb{P}$, the $N = 3$ factors, $\mathcal{P} = (\mathcal{P}^1, \mathcal{P}^2, \mathcal{P}^3)'$, follow a first-order Gaussian VAR[2]

$$\Delta\mathcal{P}_t = K_0^{\mathbb{P}} + K_1^{\mathbb{P}}\mathcal{P}_{t-1} + \Sigma\epsilon_t^{\mathbb{P}}, \quad \epsilon_t^{\mathbb{P}} \overset{iid}{\sim} N(0, I_N) \tag{1}$$

The risk-neutral factor dynamics are also given as a Gaussian VAR, but possibly with mean and persistence parameters different from its $\mathbb{P}$-measure counterpart:

$$\Delta\mathcal{P}_t = K_0^{\mathbb{Q}} + K_1^{\mathbb{Q}}\mathcal{P}_{t-1} + \Sigma\epsilon_t^{\mathbb{Q}}, \quad \epsilon_t^{\mathbb{Q}} \overset{iid}{\sim} N(0, I_N) \tag{2}$$

Market prices of risk are given as a linear function of the factors,

$$\lambda_t = \lambda_0 + \lambda_1 X_t \tag{3}$$

where the respective loadings correspond to the distance between $\mathbb{Q}$ and $\mathbb{P}$ parameters,

$$\begin{aligned} \lambda_0 &= \Sigma^{-1}\left(K_0^{\mathbb{P}} - K_0^{\mathbb{Q}}\right) \\ \lambda_1 &= \Sigma^{-1}\left(K_1^{\mathbb{P}} - K_1^{\mathbb{Q}}\right) \end{aligned} \tag{4}$$

A one-period 'shadow-rate', s_t, is specified as an affine function of factors

$$s_t = \rho_0 + \rho_1'\mathcal{P}_t \tag{5}$$

The actual observable short rate r_t is equal to the shadow rate if the latter is above a lower bound r_{LB}; otherwise the short rate sticks to that bound:

$$r_t = \max\{s_t, r_{LB}\} \tag{6}$$

Linking the short rate to the shadow rate via (6) is a technical mean to avoid the short rate going to implausibly low levels. Moreover, if the shadow rate is sufficiently far below r_{LB} and the factors driving the shadow rate are fairly persistent, then the short rate is expected to stick to the lower bound for several periods in a row. The long episodes of

[2]We follow the representation of Joslin et al. (2011), who describe the dynamics of factors with the difference in factors as the left-hand-side variable in accordance with the continuous-time analogue. Hence, the autoregressive parameters of the level representation would be given by $I + K_1^{\mathbb{P}}$.

rates staying very close to levels of zero in Japan and US suggest that this is a desirable property for a model in which rates are bounded from below.

The price at time t of a zero-coupon bond that pays off one unit of account at time $t+n$ and makes no payoff before is denoted by P_t^n. The family of arbitrage-free bond prices for all t and n is given by

$$P_t^n = E_t^{\mathbb{Q}} \left[exp \left(- \sum_{i=0}^{n-1} r_{t+i} \right) \right]. \tag{7}$$

Without the lower-bound constraint (6) bond prices would be exponentially affine functions of the factors

$$P_t^n = \exp \left(-\tilde{A}_n - \tilde{B}_n' \mathcal{P}_t \right) \tag{8}$$

where $\tilde{A}_n$ and $\tilde{B}_n$ solve the first order difference equations

$$\Delta \tilde{B}_n = K_1^{\mathbb{Q}'} \tilde{B}_{n-1} - \rho_1 \tag{9}$$

$$\Delta \tilde{A}_n = K_0^{\mathbb{Q}'} \tilde{B}_{n-1} + \frac{1}{2} \tilde{B}_{n-1}' \Sigma \Sigma' \tilde{B}_{n-1} - \rho_0 \tag{10}$$

with the initial conditions $\tilde{A}_0 = 0$ and $\tilde{B}_0 = 0$. Hence, $\tilde{A}_n$ and $\tilde{B}_n$ are functions of the model parameters $\Theta^{\mathbb{Q}} = \left\{ K_0^{\mathbb{Q}}, K_1^{\mathbb{Q}}, \Sigma, \rho_0, \rho_1 \right\}$ and time to maturity n, see e.g. Dai and Singleton (2003). Accordingly, bond yields would be affine in risk factors:

$$y_t^n = -\frac{1}{n} \ln(P_t^n) = A_n + B_n \mathcal{P}_t \tag{11}$$

with $A_n = \frac{\tilde{A}_n}{n}$ and $B_n = \frac{\tilde{B}_n}{n}$.

However, with a lower bound restriction in place, bond yields are nonlinear functions of the factors, and we denote by g_n the respective mapping from factors into yields such that the corresponding prices solve (7),

$$y_t^n = g_n \left(\mathcal{P}_t; \Theta^{\mathbb{Q}}, r_{LB} \right). \tag{12}$$

For the one-factor model ($N = 1$), g_n can be represented in closed form[3], but an exact analytical solution is not available for $N > 1$. Accordingly, one way to overcome the computational challenges of multifactor shadow-rate models is to rely on approximations.[4] Here, we resort to the pure Monte Carlo method utilized by Bauer and Rudebusch (2013), which can be summarized as follows. Given the factors $\mathcal{P}_t$ at time t, parameters $\Theta^{\mathbb{Q}}$ and the lower-bound r_{LB}, we simulate paths of the short rate $\{r_{t+1}^{(m)}, \ldots, r_{t+n-1}^{(m)}\}$ by deploying the risk-neutral factor dynamics (2) and the mapping between factors and short rates, (5) and (6). We then compute for each simulation path the expression $R_n^{(m)} = exp \left(- \sum_{i=0}^{n-1} r_{t+i}^{(m)} \right)$.

[3] See Gorovoi and Linetsky (2004) for analytical solutions for zero-coupon bonds, as well as bond options, derived with the method of eigenfunction expansions.

[4] Priebsch (2013) and Krippner (2012) develop approximations of shadow-rate multifactor models in continuous time. Wu and Xia (2014) derive similar approximations for these models in discrete time.

The solution for bond prices P_t^n in (7) is approximated by computing the average of the $R_n^{(m)}$ over $M = 5000$ simulation runs.[5]

3 Data and estimation approach

3.1 Yield curve data

The model described above holds for yields of risk-free zero-coupon bonds of arbitrary maturity. As empirical counterparts, studies in the literature have generally deployed bond yields of highly-rated sovereign issuers, where zero-coupon yields for fixed maturities are usually extracted from prices of coupon-bearing bonds.[6] However, for the euro area since 1999, there is no genuine European sovereign issuer of high-rated Euro-denominated public debt. This problem is commonly circumvented by resorting to government bond yields of one single euro-area country, such as Germany, or by using synthetic yields extracted from a pool of several high-rated sovereign issuers.

One problem with relying on German data is that during the global financial crisis and the euro area sovereign debt market crisis, German government bond yields have been frequently decreasing considerably, owing to the save-haven status of German Bunds. Such safe-haven flows have the potential to compress German yields below those levels that would reflect purely future short-rate expectations and corresponding term premia. Using, alternatively, synthetic yields based on all AAA-rated issuers suffers from similar shortcomings but is additionally challenged by the fact that the pool of AAA sovereigns can be changing and has in fact shrunken during the sovereign debt crisis, see, e.g., ECB (2014a).

As a consequence, the yield measures chosen in this paper are not based on bonds, but rather rely on overnight indexed swap (OIS) rates, based on EONIA (the overnight unsecured overnight interbank rate in the euro area). These swap rates exist for various maturities and the market has become very liquid recently, also for longer maturities. Overall, OIS rates have started to increasingly be considered as proxies for risk-free rates.[7]

[5] To put into perspective the accuracy of our Monte Carlo method, we cross-checked its outcome when applied to the Gaussian model where the analytical exponentially affine solutions exist. For the ten-year yield, the discrepancy (RMSE) between the Monte Carlo outcome and the analytical solution is not more than 0.2 bps. For yields with smaller maturities differences are smaller.

[6] See, e.g., BIS (2005) on the methodologies used by thirteen central banks to derive zero-coupon yield curves.

[7] For instance, ISDA (2014) documents in their annual survey the continuously increased use of the OIS rate as the interest rate on cash collateral pledged in Over the Counter (OTC) collateralized derivatives. See also ECB (2014a) for a discussion on the appropriate choice of a proxy for the 'risk-free' yield curve within the euro area, eventually drawing the conclusion that "The development of the OIS market provides an alternative way of measuring euro area risk-free rates".

As quoted OIS rates have essentially the interpretation of a par-bond yield[8], we use respective conversions to zero-coupon rates.

Specifically, our core data set comprises end-of-month observations of zero-coupon OIS rates for eight maturities (3 and 6 months, 1, 2, 3, 5, 7 and 10 years) from January 1999 to April 2014. That is, we have $T = 184$ monthly observations of $K = 8$ points of the yield curve. Figure 1 shows our yield data.

[Figure 1 about here]

As changes in policy rates are an important driving force for the yield curve, especially at the short end, Figure 2 shows the developments in main ECB policy rates – the main refinancing operations rate (MRO rate) and deposit facility rate (DF rate)[9] – as well as the monthly average of EONIA over our estimation period. Until January 2009, for most of the time, EONIA tended to range near the MRO rate, while since February 2009, EONIA was ranging closer to the DF rate. The latter pattern has been associated with a situation of high excess liquidity, where banks in the EONIA panel have been willing to lend overnight to other banks at a small spread over the DF rate.[10] The upshot for the analysis of the term structure of OIS rates is that there is – especially in the current low-rate environment – no simple one-to-one relation between policy rates and money market rates.

[Figure 2 about here]

For estimating the model (see section 3.3 below), we will cut the sample into two parts: one ranging from 1999 to September 2011 (153 observations), the other from October 2011 to April 2014 (31 observations). We will refer to the second subsample as the lower-bound (LB) period/sample, and the first subsample as the pre-lower-bound (pre-LB) period. The choice of the break is motivated by the fact that the ECB cut in November 2011 its DF rate to the level of 50 bps and never increased since then. Because EONIA and short-term maturity rates were already on a descending trend in October 2011 and because of fear of

[8] See Lando (2004)

[9] MRO rate and DF rate constitute – together with the marginal lending facility rate (MLF rate, not in the picture) – the key monetary policy rates of the ECB. The MRO rate is the interest rate, at which counterparties can obtain financing in the ECB's regular one-week operations against collateral. Since 8th October 2008, these have been conducted as full allotment at fixed rates, i.e. counterparties could get ECB funding at these rates at any desired scale (provided they pledge sufficient collateral). The DF rate is the remuneration for counterparties' accounts with the Eurosystem that exceed their reserve requirements (excess liquidity). Finally, the MLF rate is the rate, at which counterparties can obtain overnight funding from the Eurosystem. Usually, the DF rate and the MLF rate constitute the lower and upper bounds, respectively, of a corridor for EONIA. See [add reference]

[10] ECB (2014b) describes the recent development in excess liquidity and its interplay with money market rates.

contaminating the estimation procedure with observations belonging already to the 'lower-bound' period, we precautionarily terminate the pre-LB period with the observation of September 2011.

3.2 State space representation

For estimation purposes, the model is cast into state space form. The transition equation is given by the linear Gaussian factor dynamics under the $\mathbb{P}$ measure, (1),

$$\mathcal{P}_t = K_0^{\mathbb{P}} + \left(I_N + K_1^{\mathbb{P}}\right)\mathcal{P}_{t-1} + \Sigma\epsilon_t^{\mathbb{P}}, \quad \epsilon_t^{\mathbb{P}} \overset{iid}{\sim} N\left(0, I_N\right) \tag{13}$$

where y_t^o denotes the measurement vector $y_t^o = (y_t^{3M,o}, \ldots, y_t^{10Y,o})'$ of eight yields observed at time t. The measurement equation equates the observed data to their model-implied counterparts and an additive measurement error. As usual, the measurement error captures approximation errors in the sense that the data are not necessarily ideal representatives of risk-free zero-coupon yields, but the measurement errors also serve as residuals in a wider sense. For simplicity and parsimony, we [currently] assume that the measurement errors have the same variance across maturities:

$$\begin{pmatrix} y_t^{3M,o} \\ \vdots \\ y_t^{10Y,o} \end{pmatrix} = \begin{pmatrix} g_{3M}\left(\mathcal{P}_t; \Theta^{\mathbb{Q}}, r_{LB}\right) \\ \vdots \\ g_{10Y}\left(\mathcal{P}_t; \Theta^{\mathbb{Q}}, r_{LB}\right) \end{pmatrix} + \begin{pmatrix} \epsilon_t^{3M} \\ \vdots \\ \epsilon_t^{10Y} \end{pmatrix}, \quad \epsilon_t^n \overset{iid}{\sim} N\left(0, \sigma_e^2\right) \tag{14}$$

with g_n as defined in (12) above.

The presence of the lower-bound constraint and the resulting nonlinear pricing relation gives rise to a nonlinear measurement equation. The standard affine model, by contrast, leads to a linear measurement equation

$$\begin{pmatrix} y_t^{3M,o} \\ \vdots \\ y_t^{10Y,o} \end{pmatrix} = \begin{pmatrix} A_{3M} \\ \vdots \\ A_{10Y} \end{pmatrix} + \begin{pmatrix} B_{3M,1} & B_{3M,2} & B_{3M,3} \\ \vdots & \vdots & \vdots \\ B_{10Y,1} & B_{10Y,2} & B_{10Y,3} \end{pmatrix} \begin{pmatrix} \mathcal{P}_t^1 \\ \mathcal{P}_t^2 \\ \mathcal{P}_t^3 \end{pmatrix} + \begin{pmatrix} \epsilon_t^{3M} \\ \vdots \\ \epsilon_t^{10Y} \end{pmatrix} \tag{15}$$

with A_n and B_n given by (9), (10) and (11) above.

3.3 ML estimation and non-linear filtering

For estimating the SRTSM, we take essentially the same approach as in Bauer and Rudebusch (2013), but we deviate from them in that we also estimate the lower bound r_{LB} rather than assuming it to be fixed at zero.

In a first step, we estimate a standard three-factor affine model over the pre-LB subsample. As expounded in Bauer and Rudebusch (2013), the underlying assumption is that the shadow-rate model – and, in particular, the same parameterization – holds throughout the whole sample. We then take advantage of the fact that when the short rate is sufficiently distant from the lower bound, which we argue is the case for our pre-LB period,

the model behaves almost like its standard affine counterpart, so that the nonlinearity induced by the lower-bound constraint can be ignored.

This allows to proceed with the estimation approach put forward in Joslin et al. (2011). The state space representation described above is required since the three latent factors constructed as portfolios of yields are priced with measurement error.[11] They are constructed from the model-implied yields as portfolios in the same way as principal components are constructed from observed yields.[12] The set of parameters for which we derive estimates is $\Theta = \left(K_0^{\mathbb{Q}}, K_1^{\mathbb{Q}}, K_0^{\mathbb{P}}, K_1^{\mathbb{P}}, \Sigma, \rho_0, \rho_1, \sigma_e\right)$.[13] The initial starting values for the parameters are given by the estimation results of the case when the portfolios of yields are not purged with measurement errors.[14] Because these are good starting values, converging to the global optimum requires less than three minutes.

In the second step, we take the parameters obtained in the first step as given and estimate the lower-bound parameter r_{LB} by maximising the likelihood corresponding to the yields in the LB sub-sample. Specifically, we run the extended Kalman filter for the whole sample on the nonlinear state space model (13)-(14). This gives approximate one-step ahead forecast errors and corresponding variance-covariance matrices, which in turn allows to construct an approximate log likelihood[15]

$$\ln \mathcal{L}\left(\mathcal{Y}_T^o; \hat{\Theta}, r_{LB}\right) = \sum_{t=1}^{T} \ln p\left(y_t^o | \mathcal{Y}_{t-1}^o; \hat{\Theta}, r_{LB}\right) \tag{16}$$

where $\mathcal{Y}_t^o = (y_1^o, \ldots, y_t^o)$. Of the full likelihood, we only use that part belonging to the lower-bound period and maximize it with respect to r_{LB}, i.e.

$$\hat{r}_{LB} = \arg\max_{r_{LB}} \sum_{t=t^*}^{T} \ln p\left(y_t^o | \mathcal{Y}_{t-1}^o; \hat{\Theta}, r_{LB}\right), \tag{17}$$

where t^* is the start of the LB period. As this maximisation is over the single parameter r_{LB} only, we use a grid-search procedure over the interval from -50 bps to 20 bps.[16]

In a third step, now given an estimate of the full parameter vector (Θ, r_{LB}), we filter out the risk-factors by applying the extended Kalman filter to the non-linear state space model over the full sample period 1999 to April 2014.

[11] This corresponds to the RKF case of Joslin et al. (2011).

[12] Let $\mathcal{P}_t^o$ denote the principal components constructed from observed yields through the weighting matrix W, $\mathcal{P}_t^o = W y_t^o$. Then $\mathcal{P}_t$ are constructed from the vector of model-implied yields y_t through the same weighting matrix W, i.e. $\mathcal{P}_t = W y_t$.

[13] The actual set of parameters being estimated is $\Theta^{\mathcal{P}} = \left(\lambda^{\mathbb{Q}}, k_\infty^{\mathbb{Q}}, K_0^{\mathbb{P}}, K_1^{\mathbb{P}}, \Sigma, \sigma_e\right)$. See Theorem 1 of Joslin et al. (2011) for more details. Estimates for parameters of the set Θ are derived from the set $\Theta^{\mathcal{P}}$ through several computational steps as indicated in the same paper.

[14] This corresponds to the RPC case of Joslin et al. (2011).

[15] See Harvey (1990) and Appendix [to be done] for more details.

[16] Specifically, we compare the likelihood function for values of the parameter $r_{LB} \in \{-50, -20, -15, -10, -5, -2, 0, 2, 4, 5, 6, 8, 10, 12, 14, 15, 16, 18, 20\}$ bps. [The grid could be further refined].

4 Estimation results

4.1 Parameter estimates and interpretation of the lower-bound parameter

Table 1 displays the (approximate) ML estimates of the parameters Θ, together with their standard errors. The parameters imply a long-run level of the short rate of 2.44%. As usual, factor dynamics are fairly persistent: under the $\mathbb{P}$ measure, the largest eigenvalue of $\left(I_N + K_1^{\mathbb{P}}\right)$ amounts to 0.97.[17] Parameters corresponding to the $\mathbb{Q}$ dynamics are more precisely estimated than their $\mathbb{P}$ counterparts, owing to the rich source of information available through the cross section – a result that is often found in the literature. The standard deviation of the measurement error is estimated as 3 bps, suggesting a satisfactory fit of the three-factor specification on average over the estimation sample. Finally, the table contains the estimated market-price-of-risk parameters λ_0 and λ_1, given by the distance of $\mathbb{P}$ and $\mathbb{Q}$ dynamics, see (4). It turns out that they are very imprecisely estimated[18], which may in part reflect the relatively low precision of the $\mathbb{P}$ parameter estimates.

[Table 1 about here]

The lower bound parameter r_{LB} is estimated as 10 bps. Figure 3 displays the likelihood for the LB subsample, as defined in (17), as a function of various levels of r_{LB}. The function is non-monotone in r_{LB} but displays a clear maximum at 10 bps. In particular, the level of the likelihood clearly exceeds the corresponding level for $r_{LB} = 0$, i.e. the 'zero lower bound'. Finally, the maximum at $r_{LB} = 10$ is higher than the likelihood for the unconstrained model (i.e the affine model with no lower bound imposed).

[Figure 3 about here]

While the mode of the empirical distribution of the one-month rate (corresponding to r_t in the model) and three-month rate (shortest maturity used for estimation) during the LB period is indeed at (close to) 10 bps, these short-term interest rates have also assumed magnitudes below 10 bps during the LB-period, see top panels of figure 4 with histograms based on daily observations. In addition, the bottom panels of the same figure 4 present 'zoomed' images of the same histograms until 20 bps.

[Figure 4 about here]

[17] The largest eigenvalue is similar in magnitude to the largest eigenvalues non-adjusted for estimation bias reported in Bauer, Rudebusch, and Wu (2012) based on US data. This indicates a potential need for correcting the small sample estimation bias.

[18] Using the delta method, having the full variance-covariance matrix of parameters available.

At first sight, the fact that actual short-term rates have occasionally fallen below the estimated 'lower bound' parameter may read in contradiction to the very concept of a 'lower bound'. In order to interpret why 10 bps is nevertheless preferred over lower magnitudes of the lower bound (and in particular a lower bound of zero) it should be recalled that the likelihood criterion is a weighted average of squared one-step-ahead forecast errors. Whenever the shadow rate is sufficiently far below the lower bound and given the persistence of the factor process, short-term forcasts of the shadow-rate process are also below the bound, and hence the one-step prediction of the short rate is (approximately) equal to r_{LB}, see figure 5.[19] Choosing a level of r_{LB} below 10 bps would result in biased forecasts for short-term rates: for instance, for $r_{LB} = 0$, the one-step-ahead forecasts of the short-term rate would systematically underpredict its actual level.

[Figure 5 about here]

Moreover, the fact that some of the sample short-term rates fall below r_{LB} is also consistent with the estimated measurement error: while for the true underlying data generating process, r_{LB} may in fact provide a strict lower bound, the presence of the measurement error makes the model interpret r_{LB} as a flexible 'trampoline-style' bottom rather than a concrete pavement. Thus, from the viewpoint of the full statistical model (including measurement error), rates have some liberty to occasionally fall below r_{LB}. Against the background of this discussion, we will sometimes refer to the estimated r_{LB} as the 'effective lower bound'.

4.2 Goodness of fit and forecast performance

For the pre-LB period (over which the parameters, except r_{LB}, are estimated), the Gaussian ATSM gives a good fit to the yield curve over time, see table 2 with respective root mean square errors (RMSEs) and figure 6a plotting the average yield curve in the sample against the average model-implied term structure based on filtered states. Running the shadow-rate model on the pre-LB period gives an almost identical fit, confirming that respecting the lower bound is less relevant in an environment with interest rates sufficiently distant from r_{LB}.

[Figure 6a about here]

[Table 2 about here]

Regarding the LB period, figure 6b and table 2 show that both models give a similarly good average fit to the yield curve, with possibly some edge of the SRTSM over the ATSM

[19] For the sake of illustrating the persistent location below zero, the picture indicates that as of mid 2012 even the 95th percentile of the six-month ahead forecast of the shadow rate is negative.

– at least based on visual inspection. The RMSE amounts to 4 bps on average for both models, which is of the same order of magnitude as the respective fitting criterion for the pre-LB period. This also implicitly supports the assumption of using the pre-LB parameter estimates for fitting also the LB period.

[Figure 6b about here]

However, the similar RMSE of ATSM and SRTSM masks a qualitatively different behavior of the two models regarding their fit of the yield curve over time. As illustrated in figure 7a the SRTSM fits a flat path of short-term rates (three-month rates in the figure) rates since the second half of 2012. By contrast, the ATSM-implied yields follow better the actual three-month yield dynamics, but the levels of the fitted values are systematically overestimating their observed counterparts. For two-year yields, also the shadow-rate model traces the dynamics of the observed yield, see figure 7b.

[Figure 7 about here]

A model fit like the Gaussian one could be a reflection of over-fitting in the sense that the filtered factors align in such a way that they trace the current movements of the observed yields, but may in turn lead to unsatisfactory predictions. Model-implied predictions of short rates are in turn important in the current context, as they are an integral part of the decomposition of observed rates and premia (see section 4.3 below).

Thus, in order to check the predictive content of the models, for the short-term (and also for longer-term) yields, we conducted a forecasting exercise to compare the two models. Given the parameter estimates obtained over the pre-LB period we forecast three-month, six-month and one-year yields for forecast horizons between three and 18 months over the LB period, i.e. from October 2011 to April 2014. Notice, however, that for the SRTSM, this is only a 'pseudo' out-of-sample exercise as the r_{LB} parameter itself is estimated using data of the LB period. We also benchmark our forecasts against random-walk predictions. The results are summarized in table 3.

[Table 3 about here]

It turns out that for the short forecast horizons of three and six months, the shadow-rate model clearly improves upon the Gaussian model and also beats the random walk, where the gain in forecasting accuracy is more distinct for shorter maturities. For forecast horizons of 9 and 12 months, by contrast, the Gaussian model appears to be slightly better. For the longer horizons of 15 and 18 months, the shadow-rate model seems to be superior once again, but the random-walk predictions are clearly preferable to both models. However, these results have to be interpreted with care as the number of forecast

months is fairly small, with only between 28 observations (for the three-month horizon) and 13 observations (for the 18-month horizon) being available for forecast evaluation.[20]

4.3 Forward and term premia

We use the estimated models, SRTSM and ATSM, to decompose the spot and forward curve into expectations components and term or forward premia, respectively. One-month forward rates h periods ahead will be denoted by f_t^h and are computed as[21]

$$f_t^h = (h+1) \cdot y_t^{h+1} - h \cdot y_t^h. \tag{18}$$

Forward premia fp_t^h are given as the difference between forward rates and the respective (physical) expectations of future short rates

$$fp_t^h = f_t^h - E_t^{\mathbb{P}} r_{t+h} \tag{19}$$

Term premia tp_t^n are the difference between bond yields and average expected future short rates, or (approximately) equivalently, as the average of forward premia until the horizon n

$$tp_t^n = \frac{1}{n} \sum_{i=0}^{n-1} fp_t^i \tag{20}$$

Figure 8, left panels, shows the decomposition of six-month forward rates, f_t^{6M} into expectations and premia, starting in 2008 in order to better 'zoom' into the LB period. While until mid-2011, the ATSM and the SRTSM exhibit similar model-based forward rates and decompositions, the two models differ for the LB period. The ATSM implies close-to-zero and occasionally negative forward rates, which are decomposed into distinctly negative short-rate expectations (about -15 bps basis points) and positive forward premia. The SRTSM, by contrast, exhibits since mid-2012 relatively constant short-rate expectations equal to the estimated lower bound of $r_{LB} = 10$ bps, which is in turn a reflection of the shadow rate being distinctly negative during this period, see figure 5 again. From the viewpoint of the model, forward premia are negligible during the LB period, i.e. forward rates are approximately equal to expectations.

As there are no directly observable counterparts to forward premia, it is difficult to judge which of the models provides a more 'reasonable' decomposition into premia and

[20] Specifically, for the three-month horizon, the first forecast is based on filtered states using information up to October 2011, so the first month *for* which the forecast is produced is January 2012. The last month being forecast is April 2014, which gives 28 months available for evaluation. For the 18-month horizon, forecasts start also in October 2011, so the first month being forecast is April 2013, providing only 13 months available for forecast evaluation.

[21] As usual, these are 'implied' forward rates: given the term structure of spot rates, they result directly from arbitrage considerations.

expectations (or if, possibly, even both models are off-track in this respect).[22] However, as evidence against the Gaussian model, it may not seem very plausible that the swap market was pricing in a negative short-term rate over a half-year horizon during almost all months since mid-2012. Moreover, the forecasting results presented above, may also suggest that the expectations component of the SRTSM may be preferable to that stemming from the ATSM. Finally, apart from the model-implied decomposition, the ATSM is probably somewhat inferior in fitting the forward rate itself: it turns out that the SRTSM fits the three-month forward rate six months ahead with a negative bias and also exhibits a lower overall RMSE in fitting it (we do not have the one-month forward rate six months ahead directly available from our data set, so the 3m-in-6m is the closest proxy to check).[23] Overall, the SRTSM's results regarding short-horizon forward premia may be considered more plausible over the LB period.

Regarding the decomposition of long-term spot rates, right panel of figure 8, there is much less dissent between the models compared to the short-term forward rate decomposition. Both models find negative term premia (up to -50 bps) for most of the time during the LB period. This agreement across the models reflects the fact that yields of longer maturity are less affected by the presence of the lower bound. That is, any discrepancy of rate decompositions for short maturities – the initial summands in (20) – will not have a large impact due to the averaging over maturities up to ten years.

[Figure 8 about here]

Finally, as a general caveat, any premia decomposition is subject to considerable parameter uncertainty (apart from the model uncertainty just discussed). In fact, given the findings in section 4.1, the difference between physical and risk-neutral parameters is estimated very imprecisely. So, in particular, zero forward premia cannot be rejected, but, at least over the LB period, close-to-zero forward premia would likewise be in line with the SRTSM point estimates.

5 Policy expectations and 'lower-bound shifts'

5.1 Conditional density of future short rates and lift-off timing

One use of terms structure models is to help central banks – as well as other public and private entities – to gauge market participants' views of future interest rate developments. This is especially important at times when central banks communicate explicitly to the public their expectations regarding the path of future policy rates. Often, such 'forward guidance' is phrased in terms of the time during which the central bank intends to keep

[22] See, e.g., Swanson (2007) on the issue of model uncertainty regarding term premia estimation.

[23] Results of that cross-check available on request.

its rates near certain low levels. In this case (but also when central banks link their communication on future policy rates to macroeconomic outcomes) it is essential for monetary policy authorities to assess the market-perceived duration of a low-rate environment. A suitable model can help to extract a rich set of information about such market assessment from the term structure of interest rates.

When we talk about assessing market participants' expectations, it is in principle preferable to use the model-based $\mathbb{P}$-measure results. However, like Bauer and Rudebusch (2013), we will use $\mathbb{Q}$ measure expectations. As one reason for doing so, it allows us to compare directly the model-based assessments on the extent and timing of future rate events with typical practitioners' assessments that are often purely based on forward rates. Secondly, forward premia are estimated very imprecisely and probably small at the current juncture, as discussed above. So whenever we mention model-implied expectations these should be understood in the risk-neutral sense, possibly incorporating (small) forward premia.

From the viewpoint of the end of our estimation sample, i.e. standing on 30 April 2014, figure 9 depicts the model-based predictive densities until 2017. For a horizon of about 1.5 years, the model reflects that the market is almost certain that interest rates stay at the lower bound, while afterwards the probabilities for a rate increase start rising. Indeed, as shown in figure 10, the probability of rates sticking to the lower bound by end-April 2015 exceeds 90%, and it is only by the end of 2016 that this probability has decreased to about 50%.

[Figure 9 about here]

[Figure 10 about here]

The Gaussian ATSM, by contrast, implies a symmetric distribution of future short rates, with relatively large probabilities of the one-month rate becoming distinctly negative, see figure 11. For instance, for the one-year horizon, that model implies that the short rate stands below -50 bps with a probability of 23%. There have been increasingly discussions about possibly negative money market rates in the euro area[24]; however, standing in April 2014, negative rates below -50 bps would have been clearly considered as too extreme a scenario to prevail in one year's time.

At the same time, the mean-reversion property of factors combined with the linear short-rate equation implies a relatively quick return to higher rates with a considerable probability: in April 2014, the ATSM assigns a chance of 29% to being above 50 bps in one year's time.

[24] A negative level of EONIA has in fact been observed for the first time at end-August 2014, when EONIA was recorded at -0.4 bps.

[Figure 11 about here]

The asymmetric distribution of future interest rates in a lower-bound situation implies that the mode and the mean of that distribution will differ. As shown in figure 9, when rates are at the lower bound, the most likely rate path going forward is below the expected rate path. For the Gaussian model, the two will necessarily coincide.

As mentioned above, the central bank and other market observers are often interested in the market assessment of the time when interest rates will exceed a certain threshold level. For instance, it might help the central bank to assess whether its communication on the extent of a low-rate period is understood by market participants. Given the estimated model, one can derive the complete distribution of the timing of any interest rate event. For instance, standing again at end-April 2014, we can use the SRTSM to estimate when the market (as reflected by the pricing of the term structure) expects the currently low interest rates to exceed again a level of 50 bps. In order to do so, one can rely on a simple Monte Carlo simulation. For each run, a realization of the short rate trajectory is produced and the time τ is recorded when r first exceeds 50 bps (and does not return below that figure for, say, six months).

Figure 12 displays the result of that exercise, i.e. the estimated distribution of the time τ when the short rate will exceed 50 bps once again, given the situation at end-April 2014. It turns out that the median of that distribution is in June 2017. That is, with a probability of 50% the 50-bps level will be reached earlier or later. The *expected* time to reach that level is even much later, namely in February 2018. Thus, it is expected for interest rates to take more than 3 years to revert to a level of 50 bps.

[Figure 12 about here]

How does that result compare to the timing that one would infer from the forward curve? Following that simple approach, one would intersect the forward curve with the respective rate threshold (here 50 bps) and read off the respective timing from the horizon axis. As visible from figure 9, this would correspond to June 2016, i.e. it is about a year earlier than what is implied by the analysis described before.

Why does the time τ^* satisfying $E_t(r_{\tau^*}) = 50$ bps (i.e. the forward curve crosses the threshold) underestimate the model-implied median timing? A useful way to think about this is via the shadow-rate process, as expounded in Bauer and Rudebusch (2013). As the threshold of 50 bps is above the lower bound, the event of the short rate path r crossing 50 bps is equivalent to the event of the shadow rate s crossing that level. The time when the median of the shadow rate distribution equals 50 bps is approximately the time that corresponds to the median of the distribution of the crossing times: when the median of the shadow rate distribution is at 50 bps, it implies that – think in simulation outcomes – at least 50% of the possible realisations of the shadow rate are above 50 bps, which in

turn implies that at least 50% of the shadow-rate trajectories must have crossed the 50 bps level.[25] Due to the symmetry of the Gaussian shadow-rate distribution its median is equal to its mode and its expectation. So the median crossing time is approximately equal to the time $\bar{\tau}$ when the mode, the median and the expectation of the shadow rate is at 50 bps.

Now, for the time τ^*, where $E_t(r_{\tau^*}) = 50$ bps, we have $E_t(s_{\tau^*}) < 50$ bps.[26], so the median shadow rate is also below 50 bps at time τ^*. That is, at τ^* more than half of the trajectories have not reached the 50 bps level, hence the point were the forward rate crosses 50 bps tends to underestimate the median timing.

At the same time, the *mode* of the shadow rate distribution (again, equal to mean and median) equals the mode of the short-rate distribution at 50 bps. Hence, as a corollary of the above explanation, the time horizon where the most likely ('modal') path of the short rate crosses the threshold, corresponds approximately to the median crossing time.

As shown in figure 13, since mid-2012 the estimated median timing when future one-month rates would return to 50 bps has been ranging between about 25 and 40 months. The corresponding simple metric implied by the respective forward curve crossing that level has always implied an earlier timing of between 5 to 15 months before the model-implied median date.

[Figure 13 about here]

5.2 Shifting the lower bound even lower

Jumping from end-April 2014 (the end of our estimation sample) to end-June 2014, the yield curve ranges now much lower than its end-April counterpart, see figure 14. A main factor for this lower positioning of the term structure was certainly the cut in key ECB interest rates decided on 5 June 2014. The MRO and DF rate were cut from 25 and 0 bps to 15 and -10 bps, respectively. Compared to end-April, the short end of the curve has come down less strongly than the long end and the June curve is very flat until a maturity of about two years, exhibiting a level of about 5 bps over that maturity range.

[Figure 14 about here]

The spot curve (and likewise the corresponding forward curve) being very flat within the initial maturity spectrum is indeed a key feature implied by SRTSMs, for which the lower bound constitutes an absorbing state. So the end-June yield curve after the rate cut may well be described by our SRTSM. However, after the rate cut, our estimated effective lower bound of 10 bps would no longer be applicable and the end-June curve

[25] [Explain why this is only approximation]

[26] The expectation of the shadow rate is always smaller than that of the short rate. [Explain]

rather reflects a level of around 5 bps for the lower bound. In fact, this is also in line with short-term money market rates hovering around a level of about 4-5 bps between 5 June and end-July, see figure 15.

[Figure 15 about here]

From the SRTSM perspective, the June rate cut can arguably be interpreted as a constellation where the lower bound itself has been shifted. This is a rather unusual feature compared to what is empirically analyzed in the literature on the term structure at the lower-bound and, specifically, on shadow-rate models. Usually, the lower-bound model is applied to a situation where short-term policy rates have reached the (perceived) lowest level. Short-term market rates are expected to move in similar territory for some prolonged time and then at one point move up, but not further down. The analysis of the previous subsection focusing on the situation of end-April 2014 gave indeed a picture along these lines: the model foresees a long period of short rates sticking near the lower bound and it was only in about two years that a lift-off from the lower bound was priced in with a probability of more than 50%. So one careful interpretation is that market participants, for all practical purposes, were indeed pricing in an effective lower bound of 10 bps for the time until April 2014.[27] Accordingly, they needed to adjust their lower-bound perception downwards in light of the policy rate cut.[28]

Against this background, the lower bound itself may be interpreted as a (changeable policy) parameter, and we look at the corresponding comparative statics: how does the term structure of one-month forward rates change if the lower bound is changed by a marginal amount. For this analysis, we use the approximation formula[29] provided in Wu and Xia (2014):

$$f_t^h \approx r_{LB} + \sigma_h^{\mathbb{Q}} \cdot g\left(\frac{E_t^{\mathbb{Q}}(s_{t+h}) - r_{LB} - J_h}{\sigma_h^{\mathbb{Q}}}\right), \tag{21}$$

where $\left(\sigma_h^{\mathbb{Q}}\right)^2 = Var_t^{\mathbb{Q}}(s_{t+h})$, $g(x) = x\Phi(x) + \phi(x)$, with $\phi(\bullet)$ and $\Phi(\bullet)$ denoting the density and CDF of a standard normal, respectively, and J_h is a variance term, which depends on the horizon h but is independent of the factors and the lower bound.

[27] In particular, survey results from the SPF and a regular poll conducted by Reuters suggest that not more than 10% of market participants were expecting a rate cut by June.

[28] Some additional qualifications are in order, which do not affect the main line of reasoning, though. [Discuss anticipation effects]. The rate cut was very special as it brought about a negative DF rate which was unchartered territory for all market participants. So even if market players would have known about the rate cut with certanty, there would have been considerable uncertainty about the effect of the new MRO-DF rate constellation on money market rates. In fact, while they first hovered around 5 bps as described, they fell even further to around zero during August 2014.

[29] Computing the derivative in figure 16 using numerical derivatives with our simulation-based forward rates leads to virtually indistinguishable results.

Noting that $g'(x) = \Phi(x)$, the derivative of the forward rate with respect to the lower bound parameter r_{LB} is given by[30]

$$\frac{\partial f_t^h}{\partial r_{LB}} = 1 - \Phi\left(\frac{E_t^{\mathbb{Q}}(s_{t+h}) - r_{LB} - J_h}{\sigma_h^{\mathbb{Q}}}\right) \tag{22}$$

Figure 16 displays the shift in the forward curve due to the marginal increase[31] in the lower bound parameter using our estimated model parameters. As visible directly from (22), the effect of a shock to the lower bound depends on the initial constellation of the yield curve. As a first case (blue line in the figure), consider a situation where the shadow rate s_t is deeply in negative territory. Then for short horizons h, $E_t^{\mathbb{Q}}(s_{t+h}) - r_{LB}$ is likewise distinctly negative, so the normal CDF is near zero and the effect of the lower bound change on the forward curve is almost one for one. For longer horizons, the effect diminishes and $E^{\mathbb{Q}}(s_{t+h})$ eventually converges to the long-run mean of the shadow rate, so the argument of the normal CDF is positive. In the limit, the effect is positive but very small.[32] When, alternatively (green line in figure 16), the shadow rate is near its long-term mean and therefore distant from the lower bound, lower-bound changes would have a negligible impact along the whole forward curve.

[Figure 16 about here]

The effects of the spot curve can be traced in analogy. As spot rates can be written as average one-month forward rates, the term structure of derivatives with respect to the lower-bound parameter is a 'smoothed version' of figure 16.[33]

Finally, the two panels in figure 17 show a full decomposition of the discrete shift in the model-implied spot and forward curves from end-April to end-June. Specifically, for each maturity n, denote by $g^n(\mathcal{P}^A; \Theta, r_{LB}^A)$ the model-implied yield or forward rate for end-April, using the filtered factors $\mathcal{P}^A$, the lower bound $r_{LB}^A = 10$ bps and the other parameters Θ, and similarly by $g^n(\mathcal{P}^J; \Theta, r_{LB}^J)$ the model-implied yield for end-June. We decompose the total change $g^n(\mathcal{P}^J; \Theta, r_{LB}^J) - g^n(\mathcal{P}^A; \Theta, r_{LB}^A)$ as

$$\begin{aligned} & g^n(\mathcal{P}^J; \Theta, r_{LB}^J) - g^n(\mathcal{P}^A; \Theta, r_{LB}^A) \\ = \; & \underbrace{g^n(\mathcal{P}^J; \Theta, r_{LB}^J) - g^n(\mathcal{P}^A; \Theta, r_{LB}^J)}_{\text{Change in factors}} + \underbrace{g^n(\mathcal{P}^A; \Theta, r_{LB}^J) - g^n(\mathcal{P}^A; \Theta, r_{LB}^A)}_{\text{Change in lower bound}} \end{aligned} \tag{23}$$

Until a maturity of 1 year, the bulk of changes in the model-implied forward curve can be explained by the shift in the lower bound, while for longer horizons, changes in risk factors

[30] The analysis in Wu and Xia (2014) computes derivatives with respect to factors, a change in the lower bound is not analysed in their paper.

[31] So flip that around for interpreting the euro area situation between April and June, which rather reflects a down-shift in the lower bound as argued above.

[32] [To be interpreted further why shift r_{LB} also affects very long forward rates?]

[33] [To be worked out further]

explain most of the changes in forward rates. However, in the absence of a macroeconomic underpinning, the model cannot shed light on the possible macroeconomic driving forces that are reflected by these changes in factors. The impact on the spot curve is similar, with the lower-bound change having a somewhat more protracted effect also on higher maturities.

[Figure 17 about here]

Overall, the possibility of a shifting lower bound needs to be further analyzed, as sketched in the conclusion.

6 Conclusion

We have estimated a shadow-rate term structure (SRTSM) model for the euro area yield curve over the period from 1999 to April 2014. Based on the term structure dynamics during a time of historically low euro area interest rates in the last part of our sample (October 2011 to April 2014, 'lower-bound period'), we obtain an estimate of 10 bps for the effective lower bound on the short rate.

Overall, the estimated SRTSM performs well with respect to cross-sectional fit and forecast performance criteria, and it captures the salient features of euro area yield curve movements before and during the lower-bound period. During the lower-bound period – and especially from mid-2012 to early 2014 – the model is confronted with three stylized facts: first, at a certain point in time, short rates have reached an effective lower bound and then hover around this level with very little variation for a protracted period of time. Second, despite short-term spot rates stuck near the lower bound, long rates continue to fluctuate. And third, the forward (and spot) curve is very flat at short- to medium-term maturities, reflecting market expectations of rates staying near the lower bound for a considerable period ahead.

These patterns are captured by our SRTSM, and they are essentially the same stylized facts that SRTSMs for the United States or Japan had to match. However, the alleged shift in the lower bound itself (after the ECB rate cut in June 2014) is a feature that, to our knowledge, has not yet been observed or addressed in the literature before. This paper has made a first step in conducting a comparative statics exercise that shows how the forward and spot curve react to a change in the lower bound. It turns out that in a low-rate environment, a change in the lower-bound parameter induces a parallel one-to-one shift of the short end of the curve (until about 1.5 years for the spot curve in our parametrization), while longer-term maturities are affected to a decreasing extent. This comparative statics exercise essentially assumes a situation where market participants were at first pricing the term structure with full confidence into the fixed lower-bound

parameter (here $r_{LB} = 10$ bps), before switching to using the new 'lower lower bound' (here $r_{LB} = 5$ bps) thenceforth.

However, a fully coherent specification of a term structure model where the lower bound is subject to change would need to pin down a suitable (possibly discretely shifting) process for the lower bound and also take a stand on whether this would be a priced factor. Developing such ideas further is left for future research.

References

Andreasen, M. M. and Meldrum, A. (2013). Dynamic term structure models: The best way to enforce the zero lower bound. Mimeo.

Bauer, M. D. and Rudebusch, G. D. (2013). Monetary policy expectations at the zero lower bound. *Federal Reserve Bank of San Francisco Working Paper Series*, 18.

Bauer, M. D., Rudebusch, G. D., and Wu, J. C. (2012). Correcting estimation bias in dynamic term structure models. *Journal of Business & Economic Statistics*, 30(3):454–467.

BIS (2005). Zero-coupon yield curve: technical documentation. *Bank for International Settlements Papers*, 25.

Black, F. (1995). Interest rates as options. *The Journal of Finance*, 50(5):1371–1376.

Bomfim, A. N. (2003). "interest rates as options": Assessing the markets' view of the liquidity trap. *Finance and Economics Discussion Series*, 45.

Christensen, J. H. and Rudebusch, G. D. (2014). Estimating shadow-rate term structure models with near-zero yields. *Journal of Financial Econometrics*, 0(0):1–34.

Dai, Q. and Singleton, K. (2003). Term structure dynamics in theory and reality. *Review of Financial Studies*, 16(3):631–678.

ECB (2014a). Euro Area Risk-Free Interest Rates: Measurement Issues, Recent Developments and Relevance to Monetary Policy. In *Monthly Bulletin July 2004*, pages 63–77.

— (2014b). Recent Developments in Excess Liquidity and Money Market Rates. In *Monthly Bulletin January 2014*, pages 69–82.

Filipovic, D., Larsson, M., and Trolle, A. (2014). Linear-rational term structure models. *Swiss Finance Institute Research Paper Series*, 15.

Gorovoi, V. and Linetsky, V. (2004). Black's model of interest rates as options, eigenfunction expansions and japanese interest rates. *Mathematical Finance*, 14(1):49–78.

Harvey, A. (1990). *Forecasting, Structural Time Series Models and the Kalman Filter*. Cambridge University Press, Cambridge University Press.

Ichiue, H. and Ueno, Y. (2006). Monetary policy and the yield curve at zero interest: The macro-finance model of interest rates as options. *Bank of Japan Working Paper Series*, E-16.

— (2007). Equilibrium interest rate and the yield curve in a low interest rate environment. *Bank of Japan Working Paper Series*, E-18.

ISDA (2014). ISDA Margin Survey 2014.

Joslin, S., Singleton, K. J., and Zhu, H. (2011). A New Perspective on Gaussian Dynamic Term Structure Models. *Review of Financial Studies*, 24(3):926–970.

Kim, D. H. (2008). Zero bound, option-implied pdfs, and term structure models. *Finance and Economics Discussion Series*, 31.

Kim, D. H. and Priebsch, M. (2013). Estimation of multi-factor shadow-rate term structure models.

Kim, D. H. and Singleton, K. J. (2012). Term structure models and the zero bound: An empirical investigation of japanese yields. *Journal of Econometrics*, 170(1):32–49.

Krippner, L. (2012). Modifying gaussian term structure models when interest rates are near the zero lower bound. *Reserve Bank of New Zealand Discussion Paper*, 02.

Lando, D. (2004). *Credit Risk Modeling: Theory and Applications*. Princeton University Press.

Monfort, A., Pegoraro, F., Renne, J.-P., and Roussellet, G. (2014). Staying at zero with affine processes: A new dynamic term structure model. Mimeo.

Priebsch, M. (2013). Computing arbitrage-free yields in multi-factor gaussian shadow-rate term structure models. *Finance and Economics Discussion Series*, 63.

Swanson, E. T. (2007). What we do and don't know about the term premium. *FRBSF Economic Letter*, (21).

Ueno, Y., Baba, N., and Sakurai, Y. (2006). The use of the black model of interest rates as options for monitoring the jgb market expectations. *Bank of Japan Working Paper Series*, E-15.

Wu, J. C. and Xia, F. D. (2014). Measuring the macroeconomic impact of monetary policy at the zero lower bound. *Working Paper 20117*.

A Figures

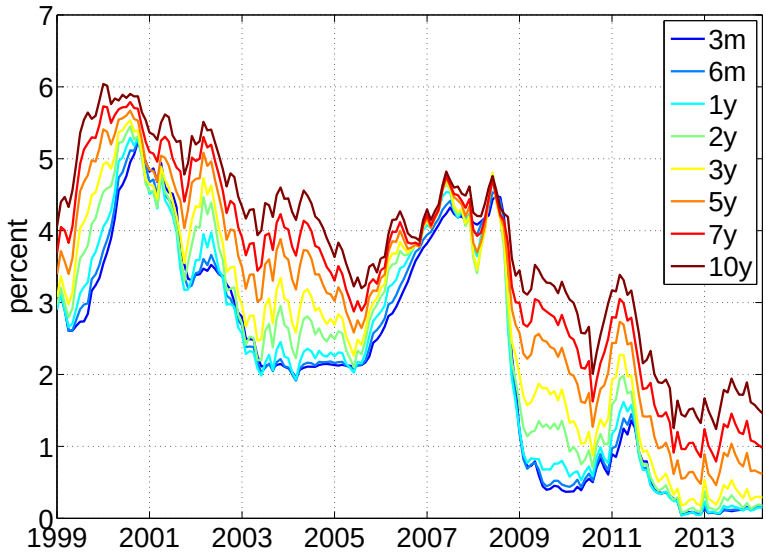

Figure 1: Zero-coupon yields derived from Overnight Index Swap (OIS) rates with the underlying rate EONIA (euro overnight index average). End-of-month data for January 1999 to April 2014 for maturities 3 and 6 months, 1, 2, 3, 5, 7 and 10 years.

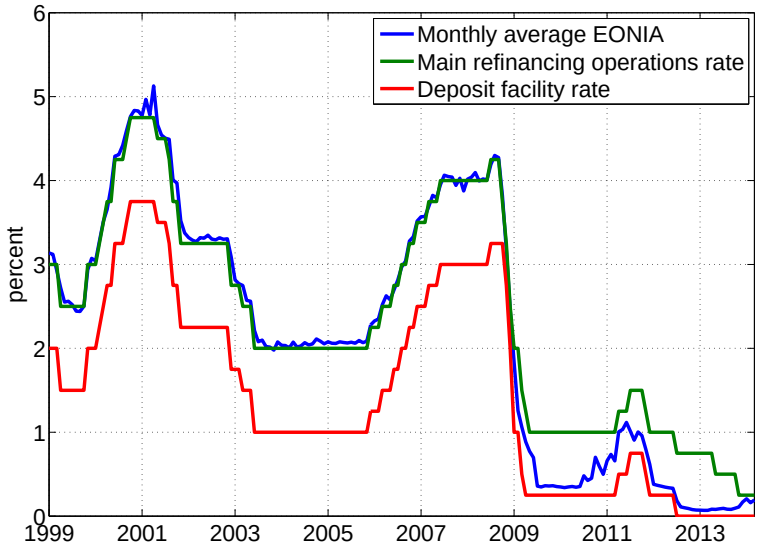

Figure 2: Time series of ECB's main refinancing operations rate and deposit facility rate for January 1999 to April 2014, together with monthly average EONIA rates for the same period.

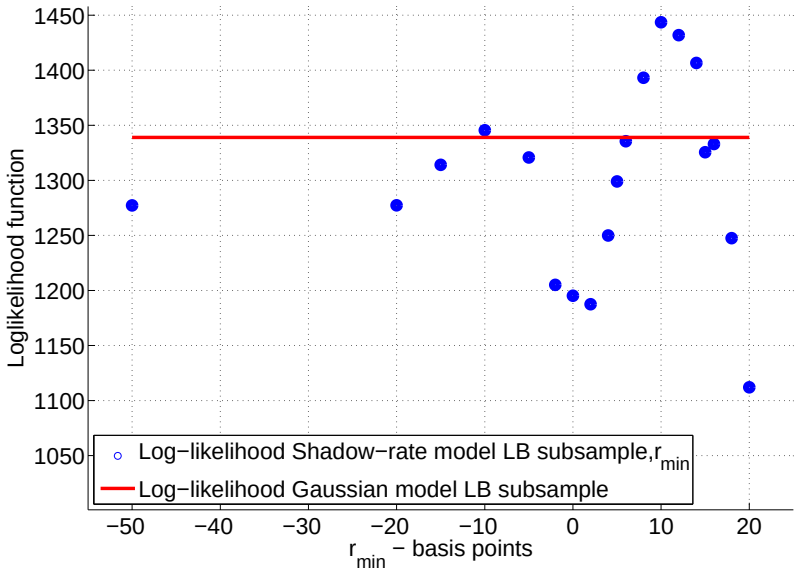

Figure 3: Loglikelihood function values corresponding to the lower-bound subsample (October 2011 - April 2014). Blue dots: loglikelihood function values for SRTSM for values of the lower-bound parameter $r_{LB} \in \{-50, -20, -15, -10, -5, -2, 0, 2, 4, 5, 6, 8, 10, 12, 14, 15, 16, 18, 20\}$ bps. Red line: value of loglikelihood for ATSM

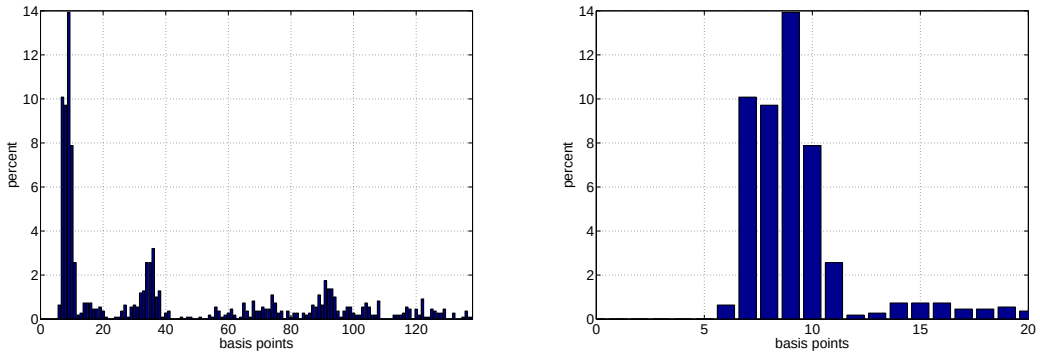

Figure 4: Histograms of the observed one-month rate for the lower-bound period (October 2011 - April 2014). Left panel: full range of realizations. Right panel: 'zoom' to 0-20 bps interval

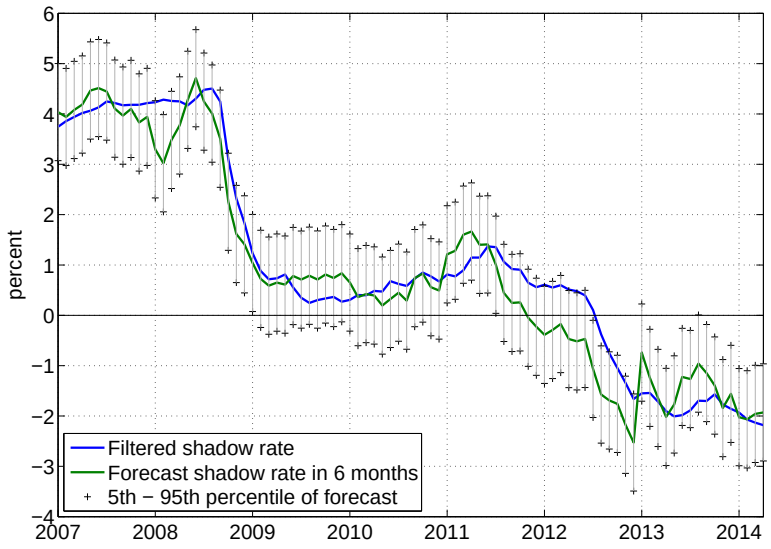

Figure 5: Filtered shadow-rate process together with six-month ahead mean forecast of the shadow rate and the 5th and 95th percentiles of the distributions of these forecasts for January 2007 - April 2014.

(a) Pre-lower bound period (January 1999 - September 2011)

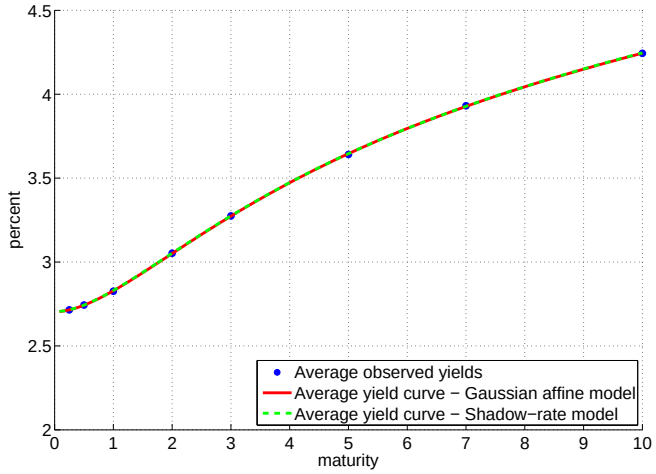

(b) Lower bound period (October 2011 - April 2014)

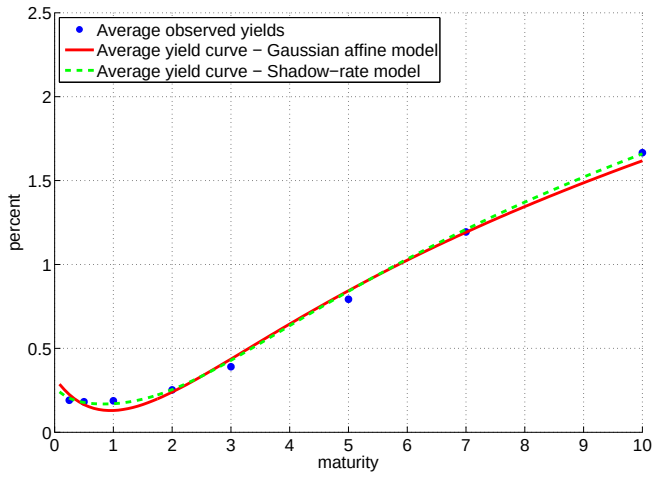

Figure 6: Comparison of selected average yields and model-implied average yield curves. Top panel presents results for the pre-lower-bound period (January 1999 - September 2011), while bottom panel for the lower-bound period (October 2011 - April 2014). In blue, mean (observed) yields for maturities 3 and 6 months, 1, 2, 3, 5, 7 and 10 years. In red, average yield curve for maturities one month until ten years derived from a three-factor ATSM. In green, average yield curve for the same maturities derived from a three-factor SRTSM with the lower bound parameter $r_{LB} = 10$ bps.

(a) Fit of the three-month yield

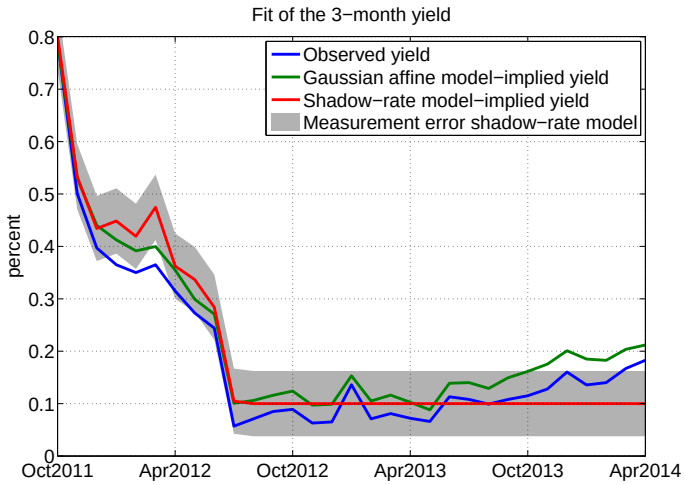

(b) Fit of the two-year yield

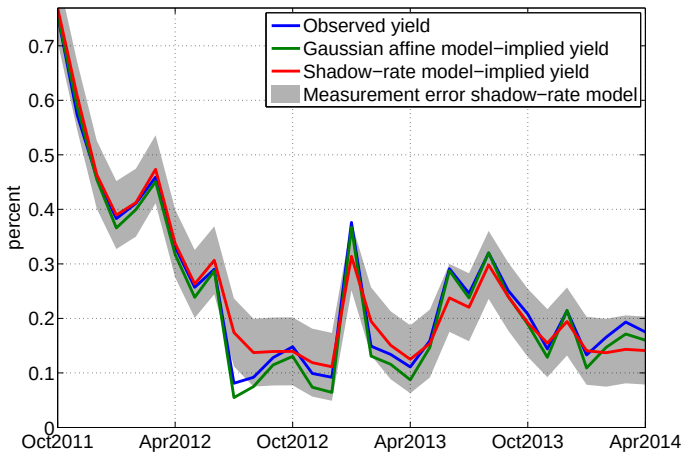

Figure 7: Time series of the observed (blue line) three-month yield and two-year yield together with the model-implied yields for the same maturities from the ATSM (green line) and the SRTSM (red line). The upper (lower) limit of the gray area represents two standard deviations of the measurement error σ_e above (below) the model-implied yield of the shadow-rate model.

(a) Decomposition six-month forward rate
Gaussian affine model

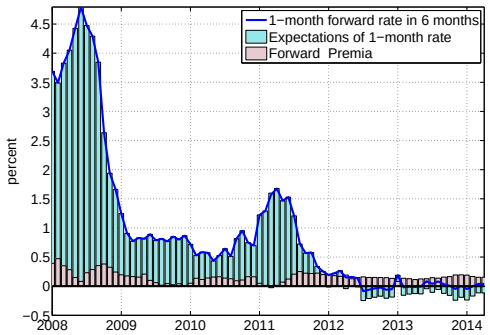

(b) Decomposition 10 years yield
Gaussian affine model

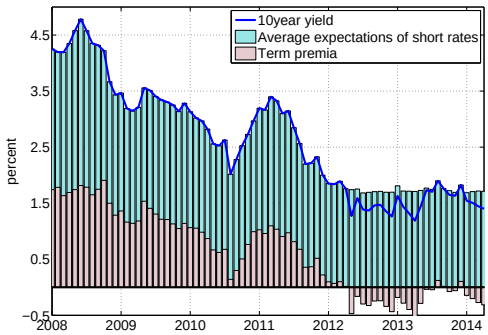

(c) Decomposition six-month forward rate
Shadow-rate model

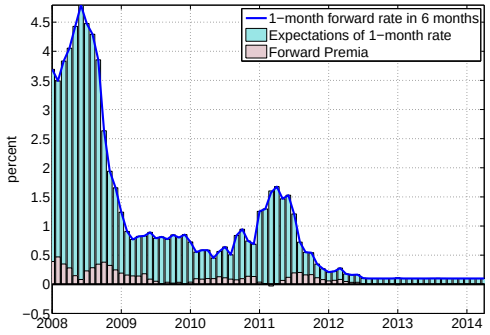

(d) Decomposition 10 years yield
Shadow-rate model

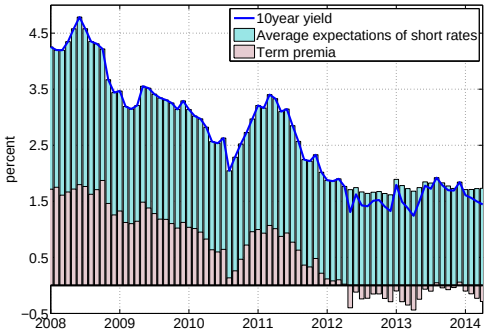

Figure 8: Forward and term premia implied by ATSM (top) and SRTSM (bottom) for the period January 2008 - April 2014. Left panels present with a continuous blue line the time series of the model-implied one-month forward rates in six months. The light blue bars represent the model-implied expectation component of each of these forward rates - expected short rate (maturity one-month) in six months. The light red bars represent model-implied forward premia - model-implied forward rate minus model-implied expectation component. Right panels indicate with a continuous blue line the time series of the model-implied ten-year yields and with light blue bars model-implied average expected short rates (one-month maturity) over the next ten years. The difference between the former and the latter represents term premia and it is indicated with light red bars.

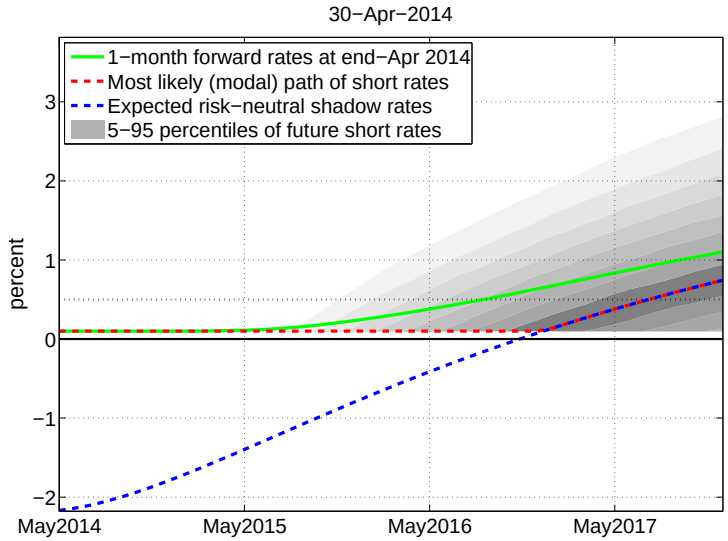

Figure 9: Conditional projection of the SRTSM until end 2017 based on information available at end-April 2014. Fan chart of risk-neutral conditional distributions of the short rate in gray. The green line represents the mean values of these conditional distributions. The dashed red line indicates the mode values of these distributions, depicting the 'modal path' of the shadow-rate. Expected future shadow-rates are indicated by a dashed blue line.

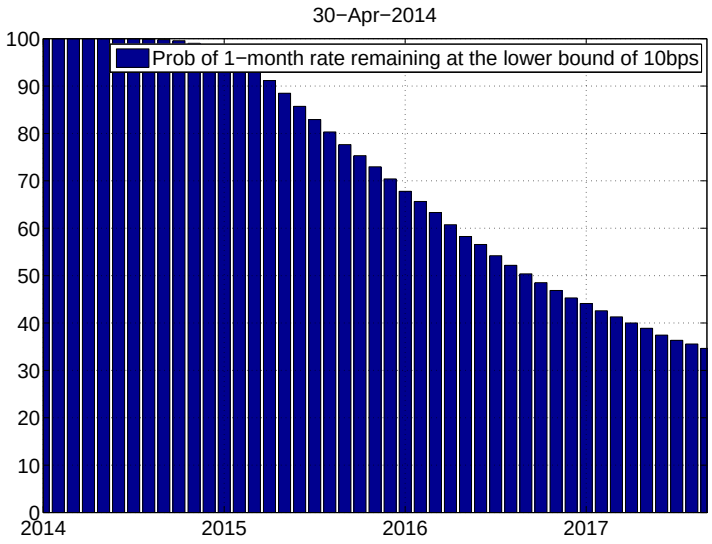

Figure 10: Risk-neutral probabilities of the short rate remaining at the lower bound r_{LB} of 10 bps until time on the x-axis. Conditional results as of end-April 2014 for the SRTSM.

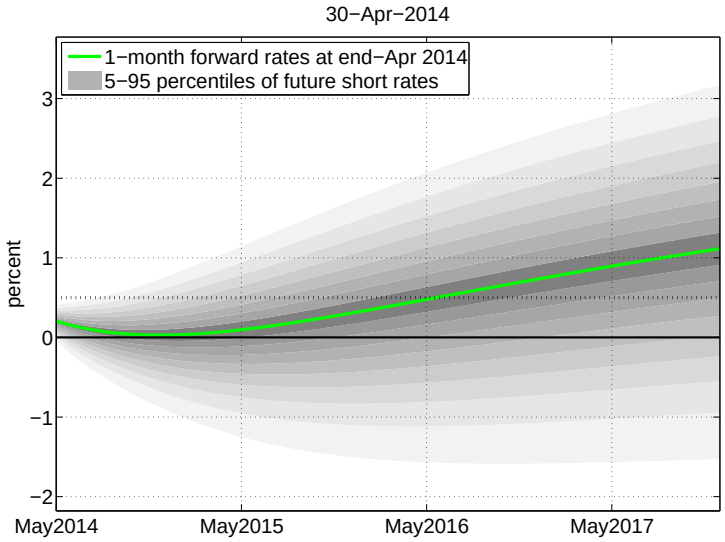

Figure 11: Conditional results of the ATSM until end 2017 based on information available at end-April 2014. Fan chart of risk-neutral conditional distributions of the short rate in gray. The green line represents the mean values of these symmetric conditional distributions.

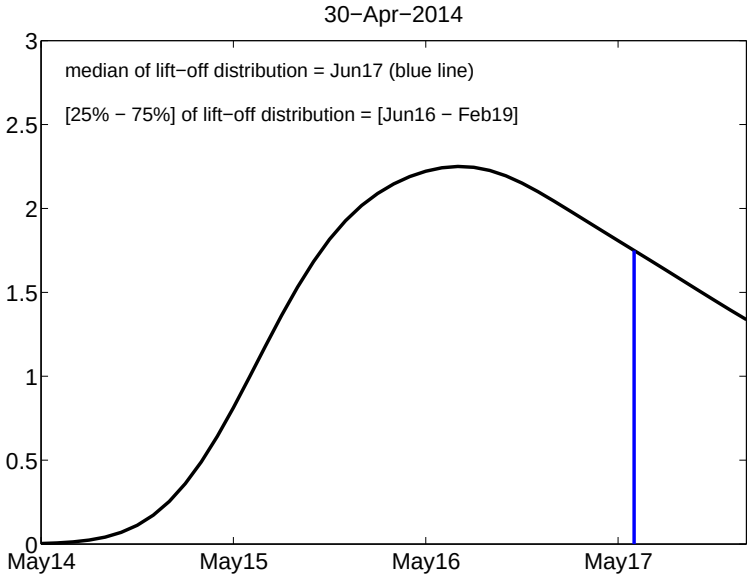

Figure 12: Distribution of the lift-off horizon conditioned on information as of end-April 2014 implied by our shadow-rate model. The risk-neutral distribution of the moment when the short-rate process will exceed the value of 50 bps set as a threshold is constructed by simulating 10000 paths of the future short rate in the SRTSM starting from April 2014. The median timing of this distribution, indicated in blue, is June 2017.

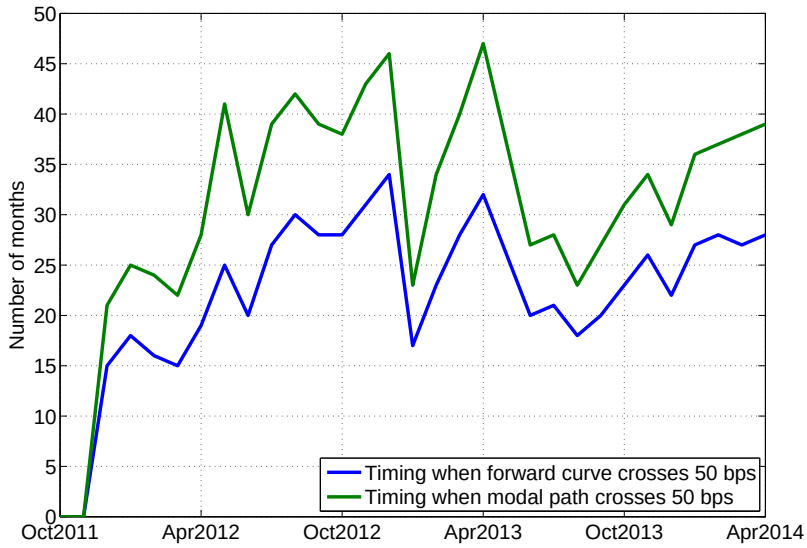

Figure 13: Time when SRTSM-implied modal path crosses 50 bps (green) vs. time when forward curve crosses 50 bps (blue). x-axis: date of modal path and forward curve; y-axis: time in months when threshold of 50 bps is crossed by modal path or forward curve, respectively, relative to that date.

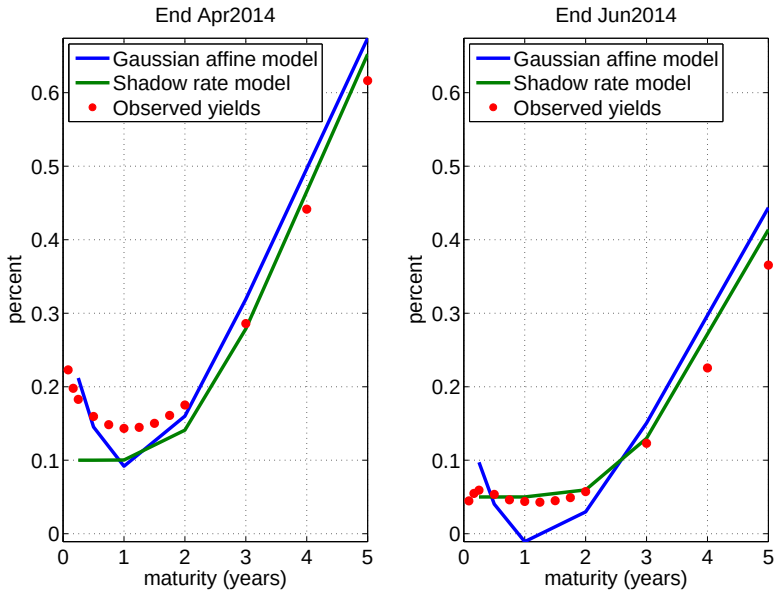

Figure 14: Model-implied yield curves until five-year maturity, together with observable yields, for end-April and end-June 2014. Left panel: SRTSM-implied yield curve with lower bound at $r_{LB} = 10$ bps. Right panel: SRTSM-implied yield curve with $r_{LB} = 5$ bps

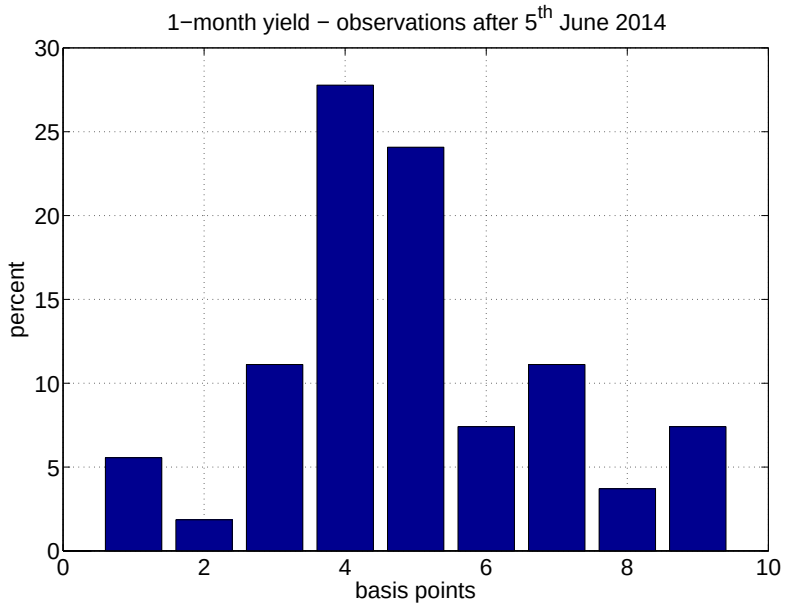

Figure 15: Histogram of observed one-month yields after the ECB rate cut in June 2014. Underlying daily data cover the period 5 June - 29 July 2014.

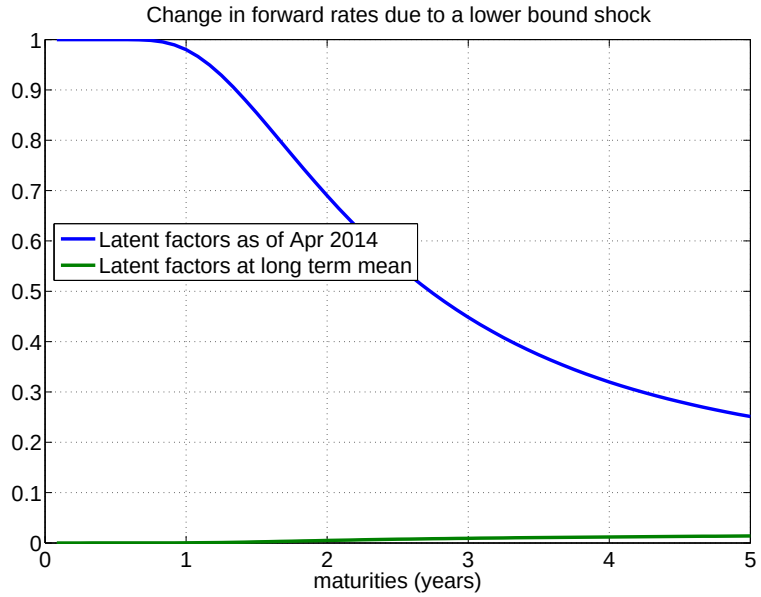

Figure 16: Derivative of one-month forward rates due to change of in the lower bound parameter r_{LB}, based on (22.

(a) Decomposing model-implied changes in yields

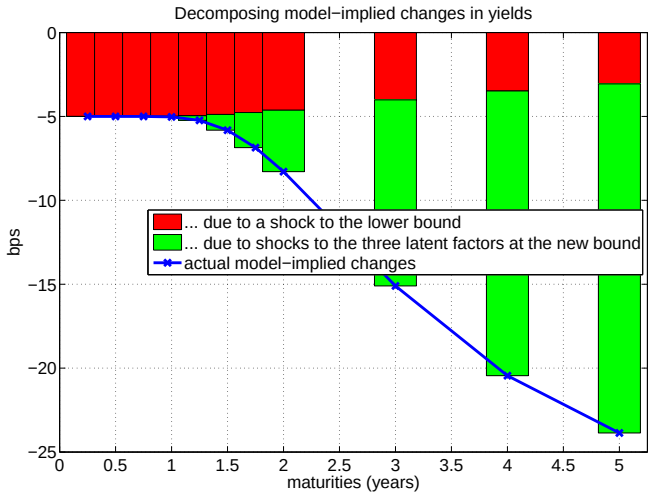

(b) Decomposing model-implied changes in one-month forward rates

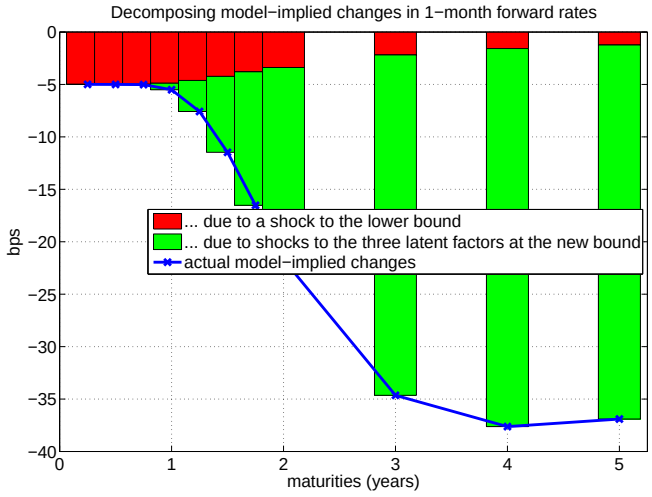

Figure 17: Decomposition of model-implied changes in the yields and in the one-month forward rates at end-June 2014 from end-April 2014 based SRTSM, following (23). Red bars: changes attributed to change in r_{LB} from 10 to 5 bps. Green bars: changes due to changes of the factors at the new lower bound, $r_{LB} = 5$ bps.

B Tables

Parameter estimates

ρ_0	- 0.0013	ρ_1	0.3989	- 0.4400	0.8626
	(0.0001)		(0.0004)	(0.0022)	(0.0110)
$K_0^{\mathbb{Q}}$	0.0065	$K_1^{\mathbb{Q}}$	- 0.0466	0.9153	- 3.4559
	(0.0005)		(0.0020)	(0.0105)	(0.0525)
	- 0.0043		- 0.0455	- 0.1687	2.7246
	(0.0004)		(0.0015)	(0.0081)	(0.0422)
	0.0051		0.0396	- 0.0711	- 1.5185
	(0.0004)		(0.0016)	(0.0085)	(0.0431)
$K_0^{\mathbb{P}}$	0.0261	$K_1^{\mathbb{P}}$	- 0.0832	0.5719	- 6.8770
	(0.0387)		(0.1832)	(1.0854)	(2.9780)
	0.0104		- 0.0540	- 0.6974	2.4793
	(0.0144)		(0.0847)	(0.4266)	(1.0435)
	0.0007		0.0869	- 0.0339	- 1.4051
	(0.0088)		(0.0428)	(0.2015)	(0.6275)
λ_0	0.3143	λ_1	-0.5862	-5.4937	-54.7568
	(0.6157)		(2.9373)	(17.3566)	(46.5136)
	0.4623		-0.0845	-19.2522	14.6961
	(0.6427)		(3.3604)	(17.8376)	(44.7747)
	-0.0641		4.3175	-4.6679	-40.9990
	(0.7795)		(3.7938)	(19.7349)	(51.5329)
σ_1	1.8038	ρ_{12}	0.4124	σ_e	0.0003
	(0.1408)		(0.0667)		(0.0000)
σ_2	0.7706	ρ_{13}	- 0.7051		
	(0.0581)		(0.0604)		
σ_3	0.3957	ρ_{23}	- 0.3906		
	(0.0286)		(0.0897)		

Table 1: Maximum likelihood parameters estimates (asymptotic standard errors) for a three-factor ATSM estimated over the period January 1999 - September 2011. Estimation based on linear Kalman filter and the normalization proposed by Joslin et al. (2011). Yields used in the estimation have maturities 3 and 6 months, 1, 2, 3, 5, 7 and 10 years. For comparability reasons, the following one-month parameters governing the dynamics of the latent factors are annualized (by multiplying by 12): $K_0^{\mathbb{Q}}$, $K_1^{\mathbb{Q}}$, $K_0^{\mathbb{P}}$, $K_0^{\mathbb{P}}$. Volatility estimates σ_1, σ_2, σ_3 of the latent factors $\mathcal{P}_t$ are annualized and expressed in percentage (by multiplying by 100*12). ρ_{12}, ρ_{13}, ρ_{23} are the correlations of the latent factors $\mathcal{P}_t$. σ_e represents the volatility of the measurement errors, identical for all maturities used for estimation. Asymptotic standard errors are computed based on the inverse of the information matrix estimated using the first derivative of the likelihood function.

In-sample model performance

Pre-lower-bound period

RMSE (bps)	Average	3-mth	6-mth	1-yr	2-yr	3-yr	5-yr	7-yr	10-yr
Gaussian affine (N = 3)	**2**	2	2	4	2	3	3	1	3
Shadow-rate (N = 3, $r_{LB} = 10$bps)	**3**	3	2	4	2	3	3	1	3
Difference	**0**	0	0	0	0	0	0	0	0

Lower-bound period

RMSE (bps)	Average	3-mth	6-mth	1-yr	2-yr	3-yr	5-yr	7-yr	10-yr
Gaussian affine (N = 3)	**4**	4	2	6	2	5	5	1	5
Shadow-rate (N = 3, $r_{LB} = 10$bps)	**4**	5	3	5	3	5	5	3	3
Difference	**0**	1	1	-1	1	0	0	2	-2

Table 2: Root mean square error (RMSE) in basis points between zero-coupon yields and model-implied yields for the two subsamples. Pre-lower-bound period is January 1999 - September 2011, while the lower-bound period covers October 2011 - April 2014.

(Pseudo) Out-of-sample model performance in the LB-period

3-month yield

Model/Forecast horizon	3-mth	6-mth	9-mth	12-mth	15-mth	18-mth
Gaussian affine (N = 3)	1.6	1.1	0.6	0.8	1.3	1.9
Shadow-rate (N = 3, $r_{LB} = 10$bps)	0.5	0.4	0.7	1.0	1.4	1.8

6-month yield

Model/Forecast horizon	3-mth	6-mth	9-mth	12-mth	15-mth	18-mth
Gaussian affine (N = 3)	1.6	0.9	0.7	1.1	1.9	2.5
Shadow-rate (N = 3, $r_{LB} = 10$bps)	0.6	0.6	0.9	1.3	1.9	2.2

1-year yield

Model/Forecast horizon	3-mth	6-mth	9-mth	12-mth	15-mth	18-mth
Gaussian affine (N = 3)	1.2	0.8	1.2	1.9	3.0	3.5
Shadow-rate (N = 3, $r_{LB} = 10$bps)	0.7	0.9	1.3	1.8	2.6	2.9

Table 3: Root mean square error (RMSE) for model-based forecasts relative to Random-Walk prediction for three-month, six-month and one-year yield at various forecast horizons over the lower bound period (October 2011 - April 2014).